Presented as late breaking results contribution
21st IFAC World Congress (Virtual)
Berlin, Germany, July 12-17, 2020

Normalized Passivity Control for Hardware-in-the-loop with Contact

Christina Insam * **L.D. Hashan Peiris** ** **Daniel J. Rixen** *

* *Chair of Applied Mechanics, Technical University of Munich, 85748 Garching, Germany (e-mail: {christina.insam,rixen}@tum.de).*
** *Centre for Power Transmission and Motion Control, University of Bath, Bath BA2 7AY, United Kingdom (e-mail: L.D.H.Peiris@bath.ac.uk)*

Abstract: Mechanical contact occurs in many engineering applications. Contact dynamics can lead to unwanted dynamic phenomena in mechanical systems. Hence, it would be desirable to investigate the influence of contact dynamics on a dynamical system already in the development stage. An appropriate method is Hardware-in-the-loop (HiL) on mechanical level. However, the coupling procedure in HiL is prone to stability problems and previous studies revealed that HiL tests of systems with contact are even more challenging, as the dynamics of the investigated system change rapidly when contact occurs. Passivity-based control schemes, well-known from teleoperation, have recently been used to stabilize HiL simulations of systems with continuous dynamics. Here, we investigate the applicability of Normalized Passivity Control to HiL tests of a one-dimensional mass-spring-damper system experiencing contact. Experimental results reveal that using this kind of passivity control manages to keep the test stable and also improves the fidelity of the HiL simulation. This research is an important first step in using passivity control for stable and safe hybrid simulation of complex systems with contact using HiL approaches.

Keywords: Hardware-in-the-loop simulation, Mechatronic systems, Passivity-based control, Robust time-delay systems, Contact dynamics

1. INTRODUCTION

Testing of components is a crucial step in the development and validation process of products. Components that come into contact during use are particularly critical parts. For example, contact occurs in testing of prosthetic feet or in the dynamics between pantographs and the overhead catenary. Mathematically speaking, contact is a discontinuity in the system equations (mass, damping and stiffness matrices), which causes i.a. excitation of higher modes in the system. As numerical modeling of contact dynamics is cumbersome and hard to validate, the critical contact scenario must be tested experimentally. However, if the systems that undergo contact are too large to be tested experimentally or are not available, as they are still in the development process, pure experimental testing is not feasible. Hardware-in-the-loop (HiL) is a method that overcomes this problem. In HiL, components of large dynamical systems can be tested under realistic boundary conditions, as the surrounding structure is simulated numerically in a co-simulation. HiL can be classified depending on the information that is exchanged over the interface between the numerical simulation and the experimental part: While *HiL on signal level* is used to test e.g. control units, *HiL on mechanical level* is used to test mechanical systems by exchanging force and displacement/velocity signals (see e.g. Olma et al. (2016)). In this paper, we work with HiL on mechanical level, which we refer to as HiL in the rest of this work. Note that this technique is also often referred to as Real-Time Hybrid Simulation/Substructuring. The structure of HiL is shown in Fig. 1. The parts of the dynamical system that are very large, mainly linear and easy to model form the numerical part (in blue). The experimental part (in green) comprises the components that are difficult to model due to nonlinearities, discontinuities and/or unknown damping and stiffness characteristics. Both parts are coupled in real-time by exchanging force [1] and displacement information via a transfer system. The transfer system (in orange) is composed of an actuator and a force-torque sensor (FTS), see e.g. Saouma and Sivaselvan (2008). The real achieved displacement z' does not correspond to the commanded displacement z due to time delay in communication and the dynamics inherent to the actuator. This means that compatibility and equilibrium between the numerical and experimental part are not fulfilled and thus additional dynamics are incorporated in the coupled loop. This deteriorates the fidelity of the HiL simulation, namely how well the test replicates the true dynamic behavior of the dynamical system. These parasitic dynamics can even make the coupled loop unstable, as the time delay acts like negative damping on the coupled loop (Saouma and Sivaselvan (2008)). Note that the transfer behavior of the FTS can often be assumed ideal. Despite significant progress in control engineering, there are still many applications where instability occurs. In Insam et al. (2020), studies of a HiL system with mechanical contact revealed that the HiL test becomes unstable when contact occurs, as

[1] The interface force acts with negative sign on the numerical part following the actio-reactio principle.

Presented as late breaking results contribution
21st IFAC World Congress (Virtual)
Berlin, Germany, July 12-17, 2020

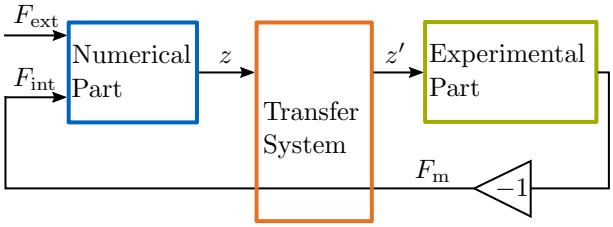

Fig. 1. Coupling of the numerical and experimental part through the transfer system in HiL. The FTS is assumed to have ideal transfer behavior.

the dynamic properties of the investigated system change rapidly at the moment of contact.

Normalized Passivity Control (NPC), proposed by Peiris et al. (2020), has recently been applied to HiL. They show that it is able to stabilize HiL systems with continuous dynamics. In the present contribution, we experimentally test the applicability of NPC to HiL tests of dynamical systems with discontinuous dynamics, more specifically, a system where contact occurs. Besides, we investigate its influence on the fidelity of the HiL test. An overview about passivity control, related work and NPC is given in the following section. In Sec. 3, the experimental setup and the parameters are given. Sec. 4 shows and analyzes the experimental results. Finally, Sec. 5 summarizes the presented results.

2. PASSIVITY CONTROL

Passivity control has its origin in teleoperation systems, where haptic devices that are in remote environments are controlled by a user, such as e.g. undersea or in space. Passivity is a sufficient criterion for stability. A system is said to be passive if the rate of change of energy inside the system is smaller than, or equal to, the power that is supplied to the system. Otherwise, the system is active, meaning that the system itself generates energy. Assembling passive systems yields a passive network. Hence, if there is one system in the network that can become active, it is sufficient to guarantee passivity of this single system in order to have a passive network.
In HiL simulations, the assembled system is composed of the numerical and experimental parts as well as the transfer system. In general, if one disregards the energy put into the system by external forces, the numerical and the experimental part are passive systems, as they consist of mechanical elements (mass, spring, damper) that cannot generate energy. However, the transfer system (actuated) can generate energy and thus become active. It has two ports, where power is exchanged: the input port that connects the numerical part to the transfer system by exchanging the desired velocity $\dot{z}$ and the measured force F_m (input power $P_\mathrm{in} = F_\mathrm{m} \cdot \dot{z}$) and the output port that connects the experimental part to the transfer system by generating the achieved velocity $\dot{z}'$ and the measured force F_m (output power $P_\mathrm{out} = F_\mathrm{m} \cdot \dot{z}'$).

2.1 Related Work

Krenn et al. (2011) were, to the authors' knowledge, the first who applied PC to HiL. They applied the so-called time domain passivity control (TDPC), which was

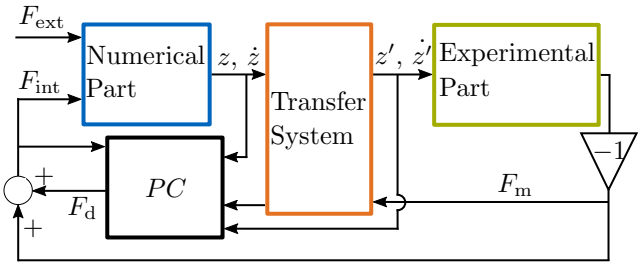

Fig. 2. Structure of NPC in HiL following Peiris et al. (2020). The passivity controller (PC, in black) augments the measured force F_m by F_d.

proposed by Ryu et al. (2004) for bilateral controllers in teleoperation systems. In the TDPC, there are two components: the passivity observer (PO) and the passivity controller (PC). The PO observes the input and output port of the possibly active system and compares the input and output energy/power. If the output energy/power is larger than the input energy/power, the PC is activated and damps the additionally added energy/power by an adaptive artificial damping α. While Krenn et al. (2011) and Peiris et al. (2018) considered the energy error to calculate the damping value α, Peiris et al. (2020) used the power error to set the damping and called the scheme Normalized Passivity Control (NPC). Ye et al. (2011) reported that using the power error has the advantages that the changes in α are smoother and that there is no integration necessary to retrieve the energy error from the power error.

2.2 Normalized Passivity Control

The scheme of NPC is visualized in Fig. 2, where the HiL structure from Fig. 1 is augmented by the PC. The PC introduces an adaptive damping force F_d if the transfer system is active i.e., $F_\mathrm{int} = F_\mathrm{m} + F_\mathrm{d}$ is sent to the numerical part. The force augmentation F_d is calculated by $F_\mathrm{d}(t_k) = \alpha(t_k) \cdot \dot{z}(t_k)$ at time t_k, where

$$\alpha(t_k) = G_\mathrm{P} \cdot \frac{\tilde{P}_\mathrm{error}(t_{k-1})}{|\tilde{P}_\mathrm{tot}(t_{k-1})|}, \tag{1}$$

$$\text{with} \quad P_\mathrm{error} = F_\mathrm{m} \cdot \dot{z}' - (F_\mathrm{m} + F_\mathrm{d}) \cdot \dot{z} \tag{2}$$

$$\text{and} \quad P_\mathrm{tot} = F_\mathrm{m} \cdot \dot{z}' + (F_\mathrm{m} + F_\mathrm{d}) \cdot \dot{z}. \tag{3}$$

The tilde operator $\tilde{\cdot}$ denotes that the signals are low-pass filtered, which smoothens the output F_d of the PC. Recommendations about the choice of the low-pass filter are given in Peiris et al. (2020). P_error and P_tot are both evaluated at time t_{k-1}. The damping scaling value G_P must be tuned by hand to achieve stability of the coupling.

3. EXPERIMENTAL SYSTEM

The dynamical system that we analyzed using HiL and NPC is a coupled mass-spring-damper system as visualized in Fig. 3. Gravity is acting in negative z-direction. The upper mass m_N is connected to the upper wall by a spring with stiffness K_p and a damper with damping constant K_d. The wall performs a sine trajectory with frequency f_d such that the lower mass m_E comes into contact intermittently. At the beginning of the experiment, the lower mass is at

Presented as late breaking results contribution
21st IFAC World Congress (Virtual)
Berlin, Germany, July 12-17, 2020

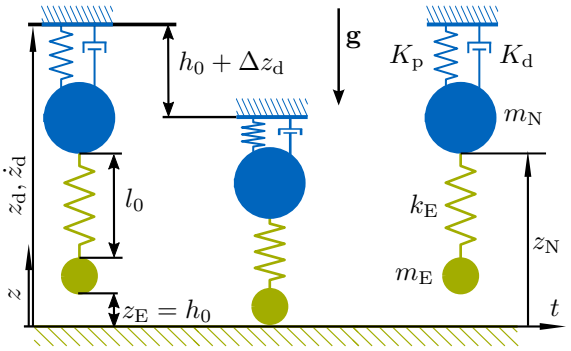

Fig. 3. The analyzed system: the numerical (blue) and experimental part (green).

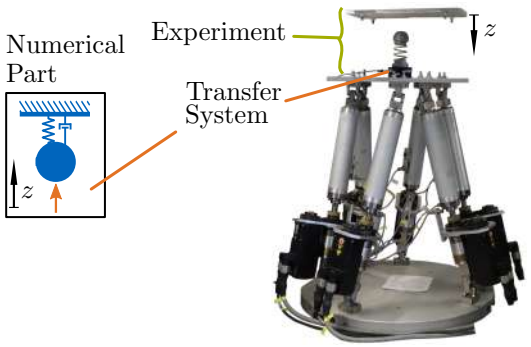

Fig. 4. Picture of the used experimental setup.

position $z_\mathrm{E} = h_0$ above the ground and the spring k_E (resting length l_0) is only loaded by $m_\mathrm{E} \cdot g$ due to gravity. The damping of this dynamical system can be varied for different experiments by changing the value K_d. Since the stability margin of a HiL test depends on the damping in the investigated system, we can change the stability margin by varying the parameter K_d. In a HiL test, one needs to define the so-called *Quantity of Interest (QoI)*, which is the outcome of the test and could be any physical quantity in the dynamical system. We chose the interface displacement z_N to be the QoI. To measure the quality of the HiL test, the real achieved interface displacement z'_N needs to be compared to a reference solution z^r_N. The reference solution is retrieved from a pure numerical simulation of the assembled system [2]. We measure the fidelity of the HiL test by taking the relative root-mean-square (RMS) error, i.e. $\frac{\mathrm{RMS}(z^\mathrm{r}_\mathrm{N} - z'_\mathrm{N})}{\mathrm{RMS}(z'_\mathrm{N})}$. If the error is small, the test is said to possess high fidelity.

The actuator that we use to move the experimental part is an in-house built Stewart platform (Fig. 4), driven by six electric motors. It is controlled with a P-PI-PI-cascade for position (P controller), velocity (PI controller), and current (PI controller). Additionally, a velocity feedforward is used to achieve better tracking performance of the actuator i.e., make z'_N follow z_N better. The implementation is done in MATLAB/Simulink (version R2016b, MathWorks) and the digital signal processor is a dSpace MicroLabBox dS1202. The sample time is set to 1 kHz ($\Delta T = 1\,\mathrm{ms}$). A six-axis FTS from SCHUNK GmbH & Co. KG is used to measure the forces.

The parameters listed in Table 1 were used to conduct the experiments. They are chosen based on experience and have no special application in mind. Depending on the damping value K_d, the HiL system is unstable ($K_\mathrm{d} = 50\,\mathrm{kg/s}$), stable ($K_\mathrm{d} = 150\,\mathrm{kg/s}$) or in the transition zone ($K_\mathrm{d} = 100\,\mathrm{kg/s}$). Note that *unstable* does not refer to unstable dynamics of the investigated dynamic system but instability that occurs in HiL due to time delay of the transfer system. We varied the damping scaling value G_P of the NPC (1) between ($0\,\mathrm{kg/s}, 4000\,\mathrm{kg/s}$) by steps of 200 to investigate its influence. The low-pass filter acting on the signals P_error and P_tot had a transfer behavior of $G_\mathrm{LP} = \frac{1}{0.01s+1}$, following Peiris et al. (2020).

[2] In general, HiL aims to investigate the behavior of unknown experimental systems. Here, however, we need a reference simulation to investigate the influence of the PC on HiL with contact dynamics.

Table 1. Parameters used for the experiments

variable	value	variable	value
h_0	0.01m	m_E	0.38 kg
l_0	0.071 m	m_N	9.62 kg
K_P	$10^4\,\mathrm{kg/s^2}$	f_d	0.25 Hz
K_d	50 kg/s, 100 kg/s, 150 kg/s	Δz_d	$0.005m$
k_E	$10^4\,\mathrm{N/m}$	g	$9.81\,\mathrm{m/s^2}$

4. EXPERIMENTAL RESULTS

We investigated the applicability of NPC to HiL with contact dynamics and the influence of NPC on the fidelity of the tests depending on the damping scaling parameter G_P. To visualize the behavior of the unstable HiL system with PC compared to the reference solution z^r_N, we show some values z'_N during one bump representative for all measurements in Fig. 5. There, the reference solution z^r_N (in black, solid thick line) and measurements from HiL tests with different values of G_P are shown. The values of G_P that are shown in the figure were arbitrarily chosen. As one can see from Fig. 5, the damping value $G_\mathrm{P} = 600\,\mathrm{kg/s}$ is not sufficient to damp the instability [3] in the system. The curves for $G_\mathrm{P} = 1800\,\mathrm{kg/s}$ and $G_\mathrm{P} = 3600\,\mathrm{kg/s}$ do not differ much, as both manage to dissipate error power.

To consider the differences more quantitatively, we investigated the resulting accumulated error energy after one bump (i.e. after 4 s), which can be seen in Fig. 6. The error energy is the sum of $\sum (P_\mathrm{out} - P_\mathrm{in}) \cdot \Delta T$ over all $n_t = 4000$ time steps. We can observe that the accumulated error energy approaches zero for higher values of G_P, meaning

[3] Here, instability means that, at least over a finite period of time, the amplitude of the oscillations increases significantly.

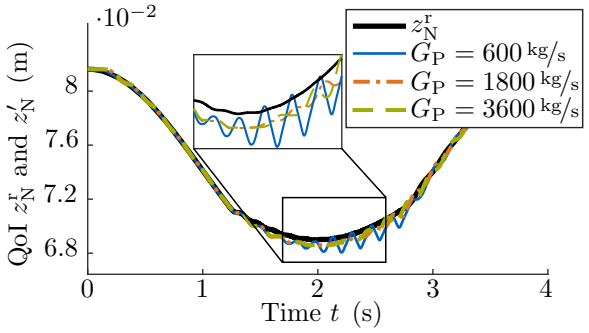

Fig. 5. The reference z^r_N and HiL solutions are shown for different G_P.

Presented as late breaking results contribution
21st IFAC World Congress (Virtual)
Berlin, Germany, July 12-17, 2020

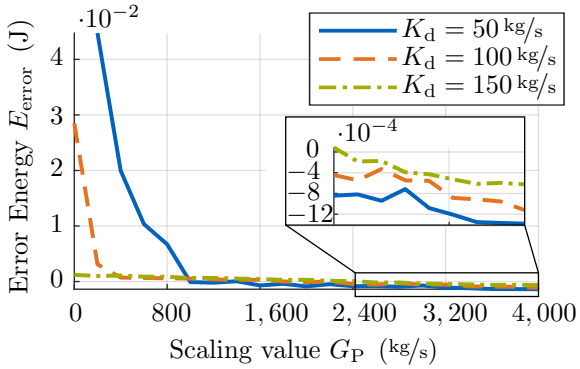

Fig. 6. The accumulated energy error after one bump for different damping ratios: $K_d = 50\,\text{kg/s}$ (blue, solid line), $K_d = 100\,\text{kg/s}$ (orange, dashed line) and $K_d = 150\,\text{kg/s}$ (green, dash-dotted line).

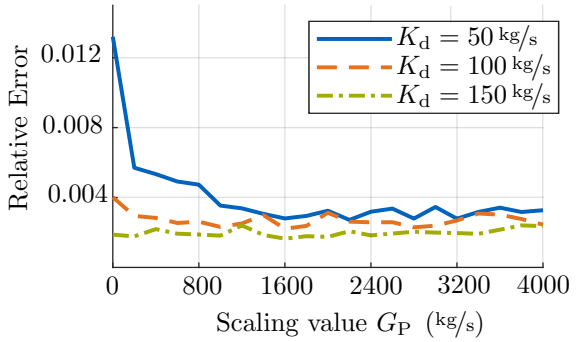

Fig. 7. The relative RMS error between the reference solution z_N^r and the solution z'_N from HiL.

that the erroneous energy introduced into the coupled HiL system decreases. For high values of G_P, in our case $G_P = 3000\,\text{kg/s}$ and higher, the error energy even reached small negative values, which shows that the passivity controller can make the system passive and even introduce slight positive damping. Further, for small damping values G_P, the error energy is larger for the unstable system ($K_d = 50\,\text{kg/s}$, in blue) than for the stable system. From the figure we conclude that in this HiL system, a scaling value larger than $G_P = 1000\,\text{kg/s}$ ensures passivity. However, the question remains what the optimum value of G_P is and whether the introduced positive damping of the passivity controller deteriorates the fidelity of the HiL test.

Hence, we calculated the relative RMS error between the reference simulation z_N^r and the achieved displacement z'_N during one bump, see Fig. 7. The error is smallest for the dynamical system that is stable without PC (green, dash-dotted line) and largest for the least damped system (blue, solid line). Nevertheless, the error decreases for the appropriate choice of damping value G_P for the unstable system. Hence, the PC improves stability and for unstable systems also fidelity of the HiL test. When G_P is increased well beyond the value needed for the HiL to be stable, we can furthermore observe a slight increase of the error for all dynamical systems, stable and unstable. This corresponds to Fig. 6, where small negative energy error values can be observed that change the investigated dynamics. For an optimum value of G_P (here $G_P \approx 2800\,\text{kg/s}$) unstable systems remain stable and reach their minimum achievable reference error. Future work will include finding strategies to determine this optimum value a priori. We want to stress at this point that the optimum value of G_P was slightly different for each experiment, depending on the noise in the whole system.

5. CONCLUSION

This paper investigates the applicability of Normalized Passivity Control (NPC) to HiL tests, where contact dynamics are involved. The results show that NPC proves successful and, with the appropriate choice of the damping amplification value G_P, the transfer system does not add erroneous energy into the HiL simulation. Furthermore, the fidelity of the test outcome increases, especially for systems that are unstable without NPC. This research suggests using NPC for stable and safe hybrid simulation of complex systems with contact. The approach could be applied to and tested for engineering applications with contact e.g., docking of satellites or testing of prosthetic feet. Future work will focus on control schemes to further improve HiL fidelity.

ACKNOWLEDGEMENTS

Preliminary work for this research was performed in the context of a student project by Doris Zhou. We thank her for the ideas and discussions.

REFERENCES

Insam, C., Bartl, A., and Rixen, D.J. (2020). A step towards testing of foot prostheses using real-time substructuring (rts). In *Special Topics in Structural Dynamics & Experimental Techniques, vol. 5*. Springer.

Krenn, R., Landzettel, K., and Boge, T. (2011). Passivity control for hybrid simulations of satellite docking. In *ICRA11 Space Robotics Workshop*.

Olma, S., Kohlstedt, A., Traphöner, P., Jäker, K.P., and Trächtler, A. (2016). Indirect force control in hardware-in-the-loop simulations for a vehicle axle test rig. In *14th International Conference on Control, Automation Robotics & Vision (ICARCV)*. IEEE, Phuket, Thailand.

Peiris, L.D.H., Plummer, A., and du Bois, J. (2020). Normalised passivity control for robust tuning in real-time hybrid tests. *International Journal of Robust and Nonlinear Control*.

Peiris, L.D.H., Plummer, A., and du Bois, J. (2018). Passivity control in real-time hybrid testing. In *2018 UKACC 12th International Conference on Control (CONTROL)*, 317–322. IEEE. doi:10.1109/CONTROL.2018.8516814.

Ryu, J., Kwon, D., and Hannaford, B. (2004). Stable teleoperation with time-domain passivity control. *IEEE Transactions on Robotics and Automation*, 20(2), 365–373. doi:10.1109/TRA.2004.824689.

Saouma, V. and Sivaselvan, M. (2008). *Hybrid Simulation: Theory, Implementation and Applications*. Taylor & Francis.

Ye, Y., Pan, Y., Gupta, Y., and Ware, J. (2011). A power-based time domain passivity control for haptic interfaces. *IEEE Transactions on Control Systems Technology*, 19(4), 874–883. doi:10.1109/TCST.2010.2062513.